

Reflectance Spectra of the 1:1 Salts of Bis(methylenedithio)tetrathiafulvalene (BMDT-TTF): Estimation of the On-Site Coulomb Energy

Michiko YOSHITAKE, Kyuya YAKUSHI,* Haruo KURODA,* Akiko KOBAYASHI, Reizo KATO,[†] and Hayao KOBAYASHI[†]

Department of Chemistry, Faculty of Science, University of Tokyo, Hongo, Tokyo 113

[†]Department of Chemistry, Faculty of Science, Toho University, Funabashi, Chiba 274

(Received November 5, 1987)

Polarized reflectance spectra were measured on the single crystals of (BMDT-TTF)AsF₆ and (BMDT-TTF)SbF₆. The charge-transfer band was observed along the stacking direction in the crystals of (BMDT-TTF)AsF₆, while in the crystal of (BMDT-TTF)SbF₆ the charge-transfer band was found not only along the stacking direction but also along the S...S direction nearly parallel to the short axis of the BMDT-TTF molecule. The effective on-site Coulomb energies and the transfer integrals of these salts were estimated by analyzing the charge-transfer bands.

Recently organic conductors based on BEDT-TTF (bis(ethylenedithio)tetrathiafulvalene) have been extensively studied, and many metallic salts have been found one after another.^{1–3)} BMDT-TTF (bis(methylenedithio)tetrathiafulvalene) is one of the derivatives of BEDT-TTF, and involves the same conjugated moiety as that of BEDT-TTF. In contrast to BEDT-TTF salts, the positive charge in BMDT-TTF radical salts tends to be localized despite two-dimensional S...S network is formed in these crystals like the crystals of BEDT-TTF salts.^{4,5)} The characteristics of such an electronic structure is probably related to the magnitude of the electron–electron Coulomb energy and the transfer integrals. In this paper, we studied the optical spectra of the (1:1) salts of BMDT-TTF, (BMDT-TTF)AsF₆, and (BMDT-TTF)SbF₆, for the purpose to characterize the dimensionality of the intermolecular interaction and of the electron–electron Coulomb interaction.

Experimental

BMDT-TTF was synthesized by the method described elsewhere.⁴⁾ Single crystals of (BMDT-TTF)AsF₆ and (BMDT-TTF)SbF₆ were prepared by the method of electrochemical crystallization in the 1,1,2-trichloroethane solutions of BMDT-TTF, (n-Bu)₄NAsF₆, and (n-Bu)₄NSbF₆ being used as electrolytes. (BMDT-TTF)AsF₆ crystallized into thin needle-like crystals elongated along the c-axis, the typical length being 1.3 mm. The single crystal of (BMDT-TTF)SbF₆ was a thin platelet developing the (100) crystal face. The crystal axes and faces were determined by the oscillation and Weissenberg photographs. The polarized reflectance spectra were measured by the use of a microspectrophotometric technique. The reflectance spectrum was measured in the spectral region from 4.2×10^3 cm⁻¹ to 25×10^3 cm⁻¹.

Results and Discussion

The crystal of (BMDT-TTF)AsF₆ belongs to the triclinic system with the space group, *P* $\bar{1}$,⁶⁾ the unit cell containing one molecule. BMDT-TTF is stacking along the c-axis with their molecular planes parallel to each other. The neighboring molecule is shifted along

the long axis of molecule, and the long axis is inclined by 34° to the c-axis. Since these molecular column is surround by AsF₆ anions, the intermolecular interaction is expected to be strongest along the c-axis. Figure 1 shows the crystal structure projected onto the (100) plane and the reflectance spectra of (BMDT-TTF)AsF₆ measured on the (100) crystal face. The dispersions of the reflectance were observed at 5×10^3 cm⁻¹, 11×10^3 cm⁻¹, and 21×10^3 cm⁻¹ in the //c spectrum. Since BMDT-TTF salt is not soluble in organic solvents, we assigned these electronic transitions by comparing with the electronic spectrum of BPDT-TTF (bis(propylenedithio)tetrathiafulvalene) salts, the cation of which involves the same conjugated moiety as BMDT-TTF. The electronic transitions of the cation radical of BPDT-TTF in the 1,1,2-trichloroethane was found at 13.5×10^3 cm⁻¹ (A), 18.4×10^3 cm⁻¹ (B), and 22.4×10^3 cm⁻¹ (C) in the visible region of the absorption spectrum.⁷⁾ Since the transition, B, is much weaker than the other transitions, the dispersion at 11×10^3 cm⁻¹ and 21×10^3 cm⁻¹ were assigned to these

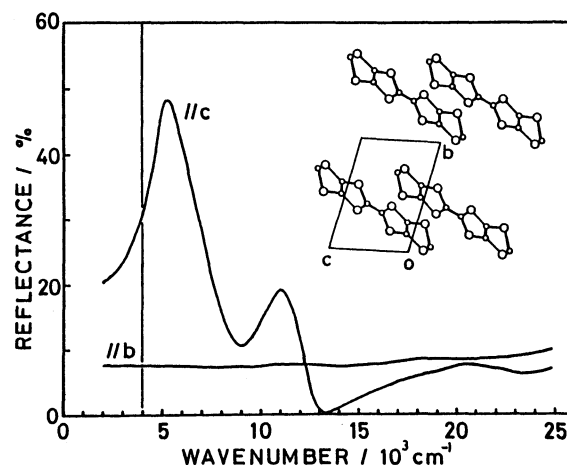


Fig. 1. Polarized reflectance spectrum of (BMDT-TTF)AsF₆ on the (100) crystal face. The reflectance curves in the region lower than 4×10^3 cm⁻¹ are the extrapolated curves by the curve fittings based on the Lorentz model. The inset shows the crystal structure projected onto the (100) plane.

intramolecular transitions, A and C, respectively. Thus, the lowest excitation at $5 \times 10^3 \text{ cm}^{-1}$ was safely assigned to the charge-transfer (CT) transition between BMDT-TTF^{+} 's. This assignment is supported by the polarization direction which is parallel to the stacking axis of BMDT-TTF . Incidentally, the intramolecular transitions in this spectral region were found to be polarized parallel to the long axis of molecule, since the short axis of the molecule is nearly perpendicular (93°) to the c-axis.

The crystal of $(\text{BMDT-TTF})\text{SbF}_6$ belongs to the triclinic system with the space group $P\bar{1}$, and $Z=1$.⁸⁾ BMDT-TTF is stacking along the b-axis such a manner as the long axis is inclined by 35° to the stacking axis. The adjacent molecule is mutually shifted to the long and short axes of molecule, so that one of the 1,3-dithiole moiety of BMDT-TTF is overlapping the same portion of the adjacent molecule. In this sense the intermolecular interaction along this stacking direction seems to be relatively weak. In contrast to the structure of $(\text{BMDT-TTF})\text{AsF}_6$ the molecular columns linked by the $\text{S} \cdots \text{S}$ interaction make a sheet parallel to the (100) plane, and several short $\text{S} \cdots \text{S}$ contacts are reported between the neighboring molecules in this sheet.⁸⁾ Figure 2 shows the crystal structures and the polarized reflectance spectra measured on the (100) and (010) crystal faces. According to the spectrum of $(\text{BMDT-TTF})\text{AsF}_6$ the intramolecular transitions at $11 \times 10^3 \text{ cm}^{-1}$ and $21 \times 10^3 \text{ cm}^{-1}$ are polarized parallel to

the long axis of molecule. Therefore, the dispersion at $11.5 \times 10^3 \text{ cm}^{-1}$ in the //a spectrum and that at $20 \times 10^3 \text{ cm}^{-1}$ in the //b spectrum are respectively assignable to these intramolecular transitions, A and C. The assignment of the $20 \times 10^3 \text{ cm}^{-1}$ transition is consistent with the observed polarization dependence, since the long axis of molecule is least inclined (35°) to the b-axis among the three crystallographic axes as shown in Fig. 2. The shoulder at $17 \times 10^3 \text{ cm}^{-1}$ in the //b spectrum probably corresponds to the weak absorption band, B, found at $18.4 \times 10^3 \text{ cm}^{-1}$ in the solution spectrum of the BPDT-TTF cation radical. From the polarization direction the strongest dispersion at $5 \times 10^3 \text{ cm}^{-1}$ in the //c spectrum is safely assigned to the CT transition between BMDT-TTF^{+} 's through the $\text{S} \cdots \text{S}$ interaction. The dispersion at $9 \times 10^3 \text{ cm}^{-1}$ in the //b spectrum looks like the intramolecular transition, A, but the excitation energy does not agree with the a-component of the transition, A. Furthermore, the width of this dispersion is slightly broader than that of the CT band in the //c spectrum. Thus we assigned this $9 \times 10^3 \text{ cm}^{-1}$ dispersion to the superposition of the CT transition along the stacking direction parallel to the b-axis and the b-component of the intramolecular transition, A, since both transitions take place most strongly along the b-axis. This assignment was confirmed by the low-temperature spectrum, because a small shoulder was found at $11 \times 10^3 \text{ cm}^{-1}$ in the //b spectrum at 42 K as shown in Fig. 3. Therefore, we arrived at the most important result in this experiment that two kinds of charge-transfer transitions were observed along the $\text{S} \cdots \text{S}$ direction as well as the stacking direction in the crystal of $(\text{BMDT-TTF})\text{SbF}_6$. Such a two-dimensional intermolecular interaction has been observed in many BEDT-TTF salts.^{9,10)} This is the first optical evidence of the two dimensionality of

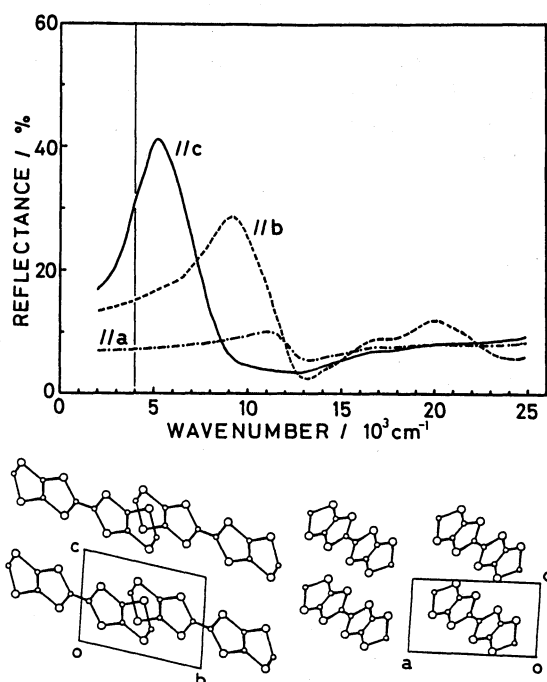


Fig. 2. Polarized reflectance spectrum and crystal structure of $(\text{BMDT-TTF})\text{SbF}_6$. The //c and //b spectra were measured on the (100) crystal face, and the //a spectrum was measured on the (010) face. The reflectance curves in the region lower than $4 \times 10^3 \text{ cm}^{-1}$ are the extrapolated curves by the curve fittings based on the Lorentz model.

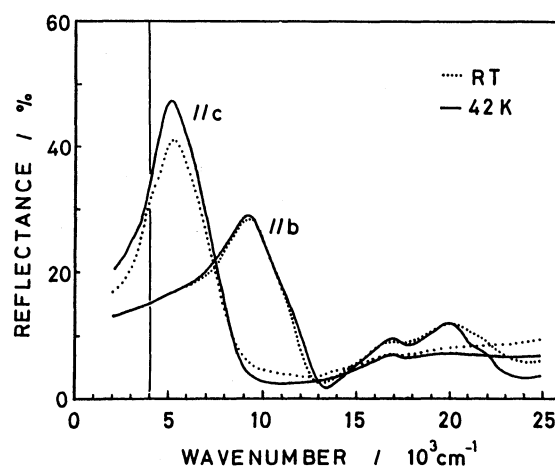


Fig. 3. Low-temperature reflectance spectrum of $(\text{BMDT-TTF})\text{SbF}_6$. The room-temperature spectrum is also illustrated by a dotted line for comparison. The reflectance curves in the region lower than $4 \times 10^3 \text{ cm}^{-1}$ are the extrapolated curves by the curve fittings based on the Lorentz model.

BMDT-TTF salts.

Figures 4a and 4b show the optical conductivity spectra of (BMDT-TTF)AsF₆ and (BMDT-TTF)SbF₆ obtained from the Kramers-Kronig transformation of the reflectance spectra. These salts have half-filled metallic band structures, if the electron-electron correlation is fully screened. However, the appearance of the CT band shown in Fig. 4 indicates the existence of a band gap. In addition, both of these salts exhibit semiconductive behavior as regards the temperature dependence of the electrical resistivity.^{6,8)} These results clearly show that the strong Coulomb interaction plays an important role in these materials. As shown in the conductivity spectrum of (BMDT-TTF)SbF₆, the CT absorption bands of the //c and //b spectra show up at different wavenumbers separating about $4 \times 10^3 \text{ cm}^{-1}$. The excitation energy of the CT band in the limit of a strongly correlated half-filled band is given by $U - V_i$, where U is the on-site Coulomb energy, V_i , the Coulomb energy between the neighboring sites along the i -th direction. The distance between the centers of adjacent molecules is 5.63 \AA along the c-axis, whereas that is 7.50 \AA along the b-axis. Therefore, the difference of the excitation energies between the CT transitions polarized along the c- and b- axes is attributed to the nearest-neighbor Coulomb interaction which depends on the distance between the adjacent molecules. The similar phenomenon was found in the single-crystal absorption

spectrum of (TTF)ClO₄, in which two charge-transfer bands separated by $3 \times 10^3 \text{ cm}^{-1}$ were interpreted to be the intra-dimer and inter-dimer CT transitions.¹¹⁾ This interpretation to the spectrum of (BMDT-TTF)SbF₆ means that the magnitude of the long range Coulomb energy is comparable to that of the on-site Coulomb energy, and thus the excited state is not the free-electron and free-hole state but the bound electron-hole state. In this situation charge-transfer process takes place predominantly between the adjacent molecules, so that the CT transition can be approximately analyzed by a dimer model. In the dimer model, the excitation energy and the oscillator strength of a CT band is represented by the Eqs. 1 and 2,¹²⁾

$$E_{CT} = U_{\text{eff}}/2 + (U_{\text{eff}}^2/4 + 4t^2)^{1/2} \quad (1)$$

$$f = (2d^2 m_e N_d / N \hbar^2) (2t^2 / (U_{\text{eff}}^2/4 + 4t^2)^{1/2}) \quad (2)$$

where E_{CT} , U_{eff} , t , f , d , m_e , N_d , and N denote the CT excitation energy, the effective on-site Coulomb energy, the transfer integral, the oscillator strength, the distance between the centers of molecules, the electron mass, the number density of a dimer, and the number density of BMDT-TTF, respectively. We set N_d/N equal to 1, since the CT interaction equivalently occurs to both side of a molecule in a regular chain. The oscillator strength, f , of the CT band was calculated by using the following equation,

$$f = (2m_e / \pi e^2 N) \int \sigma(\omega) d\omega \quad (3)$$

where e and $\sigma(\omega)$ are the charge of an electron and the conductivity spectrum, respectively. Table 1 shows the effective on-site Coulomb energy, $U_{\text{eff}} = U - V$, and the transfer integral, t , which were calculated by the use of the Eqs. 1 and 2. The oscillator strength and thus the transfer integral in the //b spectrum of (BMDT-TTF)SbF₆ is the upper limit because the b-component of the intramolecular transition is involved in the $9.0 \times 10^3 \text{ cm}^{-1}$ band. Keeping this point in mind, the relation between the transfer integral and the overlap integral is qualitatively good in BMDT-TTF salts.

Bondeson and Soos numerically examined the systematic deviation of the excitation energy and the transition probability of a CT transition in going from a dimer to a finite chain by the aid of a diagrammatic valence bond method.¹³⁾ According to their calculation, a dimer model is a good approximation to the infinite chain only for $U_{\text{eff}}/4t > 3.5$, otherwise the excitation energy predicted from a dimer model is considerably larger than that of an infinite chain. Unfortunately, the parameters, $U_{\text{eff}}/4t$, of these BMDT-TTF salt is not in the former regime, so that the actual effective on-site Coulomb energies in Table 1 is considered to be significantly larger than the values listed in Table 1. Therefore, we analyzed the CT spectrum of the one-dimensional (BMDT-TTF)AsF₆ salt by a Hubbard model, in which the long range Coulomb

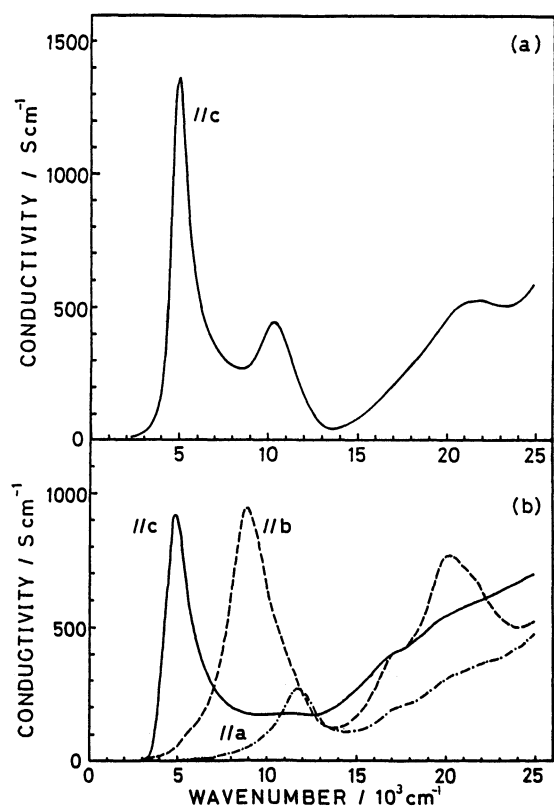


Fig. 4. Optical conductivity spectra of (a) (BMDT-TTF)AsF₆ and (b) (BMDT-TTF)SbF₆.

Table 1. Effective On-Site Coulomb Energies, U_{eff} , and Transfer Integrals, t , of (BMDT-TTF)AsF₆ and (BMDT-TTF)SbF₆ Estimated from the Dimer Model. E_{CT} and f Are the Excitation Energy and the Oscillator Strength of the Charge Transfer Band. d and S Denote the Distance between the Centers of Molecules and the Overlap Integral of the HOMO's between the Adjacent Molecules

	(BMDT-TTF)AsF ₆	(BMDT-TTF)SbF ₆	
	//c (stacking direction)	//c (S---S direction)	//b (stacking direction)
E_{CT}/eV	0.62	0.61	1.1
f	0.43	0.31	<0.60
$d/\text{\AA}$	5.84	5.63	7.50
U_{eff}/eV	0.57	0.60	1.1
t/eV	0.09	0.08	<0.11
S	-10.6×10^{-3}	-12.5×10^{-3}	-5.1×10^{-3}

energy is completely neglected. In the one-dimensional chain, the exact solutions were reported on the optical excitation energy¹⁴⁾ and the oscillator strength¹⁵⁾ as shown in the following equations.

$$E_{\text{opt}}/4t = u - 1 + 2 \int_0^\infty (J_1(x)/x) (1 + \exp(2ux))^{-1} dx \quad (4)$$

$$(f/4t)(\hbar^2/md^2) = \int_0^\infty (J_0(x)J_1(x)) [x^{-1}(1 + \exp(2ux))^{-1} + u(1 + \cosh(2ux))^{-1}] dx \quad (5)$$

where E_{opt} is the absorption edge of the optical transition across the Hubbard gap, u is defined to be $U_{\text{eff}}/4t$, and $J_0(x)$ and $J_1(x)$ are the Bessel functions. The values of $E_{\text{opt}}/4t$ and $(f/4t)(\hbar^2/md^2)$, which were obtained by numerical calculation, were plotted against u in Fig. 5 together with the quantity of $(E_{\text{opt}}/f)(md^2/\hbar^2)$ which is experimentally obtainable. We defined the absorption edge, E_{opt} , as the wavenumber at which the conductivity curve takes half of the maximum value of the CT absorption band. The parameter, $u=U_{\text{eff}}/4t$, was calculated to be 1.80 from the u -dependent curve of $(E_{\text{opt}}/f)(md^2/\hbar^2)$ by the use of the experimental values, $E_{\text{opt}}=0.56$ eV, $f=0.43$, and $d=5.84$ Å. The parameters, t and U_{eff} , were determined to be 0.14 eV and 1.0 eV from the u -dependent curves of $(E_{\text{opt}}/4t)$ and $(f/4t)(\hbar^2/md^2)$. This is the first attempt to analyze the CT band of the regular-stack one-dimensional chain with a half-filled band on the basis of the exact solution of the Hubbard model. However, the analysis is not complete, because the appearance of the two CT bands at different wavenumbers in the polarized spectrum of (BMDT-TTF)SbF₆ indicates that the nearest-neighbor Coulomb interaction should be included in the analysis. However, the theoretical study on the optical transition of the extended Hubbard model has not been conducted in the case $u \approx 1$. Bondeson and Soos numerically examined the difference of the optical

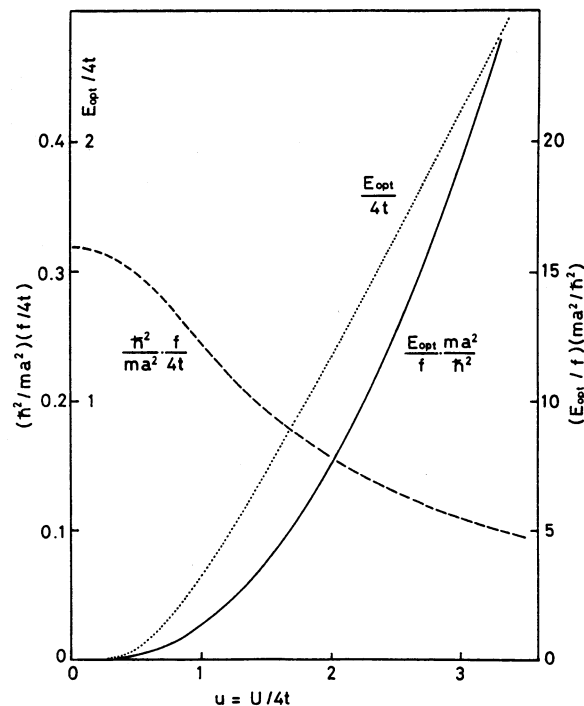


Fig. 5. Numerical calculation of the excitation energy, the oscillator strength, and their ratio which is predicted from the exact solution of the one-dimensional Hubbard model.

transition across the Hubbard gap between the extended Hubbard model and the Hubbard model. According to their calculation the excitation energy of the CT band based on the extended Hubbard model in the case $U-V_1 \approx 4t$ is significantly higher than that based on the Hubbard model in the case $U_{\text{eff}} \approx 4t$ and much lower than that of the dimer model. Therefore, we consider that the effective on-site Coulomb energy, U_{eff} , is in the range between 0.6 eV and 1.0 eV. The numerical calculation by Bondeson and Soos also indicated that the transition probability of the CT band did not change significantly among the dimer model, the Hubbard model and the extended Hubbard model, so that the transfer integral, t , was estimated to be about 0.1–0.15 eV. Torrance et al. examined the band parameters of TTF salts, (TTF)X (X=Cl_{0.80}, Br_{0.79}, and I_{0.71}).¹⁶⁾ They estimated the parameters, U_{eff} and t , to be 1.25 eV and 0.28 eV, respectively. Because they used the dimer model to obtain these parameters. U_{eff} must be larger than 1.25 eV. Therefore, we conclude that the on-site Coulomb energy of BMDT-TTF salt is significantly smaller than that of TTF salts. This is in accord with the extended molecular structure of BMDT-TTF in comparison with TTF.

References

- 1) H. Kobayashi, R. Kato, T. Mori, A. Kobayashi, Y. Sasaki, G. Saito, T. Enoki, and H. Inokuchi, *Mol. Cryst. Liq. Cryst.*, **103**, 33 (1984).
- 2) R. P. Shibaeva, V. F. Kaminskii, and E. B. Yagubskii,

Mol. Cryst. Liq. Cryst., **119**, 361 (1985).

3) J. M. Williams and K. Carneiro, *Adv. Inorg. Chem. Radiochem.*, **29**, 249 (1986).

4) R. Kato, A. Kobayashi, Y. Sasaki, and H. Kobayashi, *Chem. Lett.*, **1984**, 993.

5) R. Kato, H. Kobayashi, A. Kobayashi, and Y. Sasaki, *Chem. Lett.*, **1984**, 1693.

6) R. Kato, H. Kobayashi, and A. Kobayashi, unpublished data.

7) K. Yakushi, H. Tajima, T. Ida, M. Tamura, H. Hayashi, H. Kuroda, R. Kato, H. Kobayashi, and A. Kobayashi, *Synthetic Metals*, in press.

8) R. Kato, H. Kobayashi, and A. Kobayashi, *Chem. Lett.*, **1986**, 2013.

9) H. Kuroda, K. Yakushi, H. Tajima, and G. Saito, *Mol.*

Cryst. Liq. Cryst., **125**, 135 (1985).

10) H. Tajima, H. Kanbara, K. Yakushi, and G. Saito, *Solid State Commun.*, **57**, 911 (1986).

11) K. Yakushi, S. Nishimura, T. Sugano, H. Kuroda, and I. Ikemoto, *Acta Crystallogr., Sect. B*, **36**, 358 (1980).

12) M. J. Rice, *Solid State Commun.*, **31**, 93 (1979).

13) S. R. Bondeson and Z. S. Soos, *Chem. Phys.*, **44**, 403 (1979).

14) A. Mursurkin and A. A. Ovchinnikov, *Soviet Phys. Solid State*, **12**, 2031 (1971).

15) D. Baeriswyl, J. Carmelo, and A. Luther, *Phys. Rev. B*, **33**, 7247 (1986).

16) J. B. Torrance, B. A. Scott, B. Welber, F. B. Kaufman, and P. E. Seiden, *Phys. Rev. B*, **19**, 730 (1979).
